Werk

Jahr: 1977
Kollektion: fid.geo
Signatur: 8 Z NAT 2148:
Digitalisiert: Niedersächsische Staats- und Universitätsbibliothek Göttingen
Werk Id: PPN1015067948_0043
PURL: http://resolver.sub.uni-goettingen.de/purl?PPN1015067948_0043

LOG Id: LOG_0038
LOG Titel: The inversion of long range seismic profiles
LOG Typ: article

Übergeordnetes Werk

Werk Id: PPN1015067948
PURL: http://resolver.sub.uni-goettingen.de/purl?PPN1015067948
OPAC: http://opac.sub.uni-goettingen.de/DB=1/PPN?PPN=1015067948

Contact

Niedersächsische Staats- und Universitätsbibliothek Göttingen
Georg-August-Universität Göttingen
Platz der Göttinger Sieben 1
37073 Göttingen
Germany
Email: gdz@sub.uni-goettingen.de

J. Geophys. 43, 243–256, 1977

Journal of Geophysics

The Inversion of Long Range Seismic Profiles

B.L.N. Kennett

Department of Applied Mathematics and Theoretical Physics,
University of Cambridge, Silver Street, Cambridge CB3 9EW, United Kingdom

Abstract. The use of controlled seismic sources has markedly improved our knowledge of the seismic structure of the lithosphere. In particular the recent use of relatively closely spaced recording stations has shown the existence of fine structure in the character of the seismic wave field.

The inversion of this detailed data has involved the use of both travel times and waveform analysis. Bounds on the velocity depth distribution may be obtained by extremal travel time inversion and then more detailed models constructed to fit the observed travel times. These preliminary velocity models are then refined by matching the character of the waveforms along the profile by comparison of the observed seismograms with theoretical seismograms calculated for the proposed models. The velocity structure thus obtained is however dependent on the attenuation structure, which creates an additional problem in the inversion.

Improved knowledge of lithospheric structure in complex areas depends on making allowances for lateral variation in crustal structure along a profile. The effect of topography at the crust-mantle interface on the seismic wave field is considered in detail.

Key words: Long range profiles – Inversion – Travel times – Waveforms – Theoretical seismograms – Attenuation – Lateral variations.

1. Introduction

The study of the uppermost part of the earth's mantle by seismic observations was begun by Mohorovičić (1910), with his work on the travel times of the Kulpatal earthquake of 1909 October 8 which lead to the suggestion of a sharp increase in velocity at a depth of about 60 km. Many further studies were made of the travel times from near earthquakes but the use of standard seismographic station records gave relatively low timing precision and a sparse recording network. This meant that the data quality was insufficient to resolve any detail in the velocity distribution. However Jeffreys (1926) was able to show that the

amplitude behaviour of the P_n phase, propagating through the upper mantle, was incompatible with a uniform medium and required the velocity to increase with depth.

Recently increasing use has been made of "controlled" sources of known time origin and location, together with a comparatively dense recording network, which has often been deployed specifically for a particular experiment. From this high quality data it is possible to begin to unveil the details of the velocity distribution in the mantle.

The first major long range controlled source experiment was the "Early Rise" experiment in 1966 when a number of five ton explosive charges were fired in Lake Superior and recorded along nine main profiles radiating from the lake across most of North America (Iyer et al., 1969). Arrivals were observed out to 2000 km and beyond. Although a very large number of stations were deployed in the field, the continent – wide scope of the experiment lead to only a reasonable station spacing on any one profile (about 50–100 km apart). The interpretation of the data has largely been based on travel time analysis (e.g. Hales, 1971) and has not always taken into account the amplitude distribution along the profile. There are also significant lateral variations in upper mantle structure across North America.

To further constrain the mantle velocity distribution Helmberger and Wiggins (1971) and Wiggins and Helmberger (1973) used recordings of nuclear tests at the Nevada test site. These records for ranges up to 25° were obtained from the uniform LRSM network of stations. An attempt was then made to match the observed seismograms with theoretical seismograms calculated for proposed velocity models. The data set was further supplemented by using earthquake sources in Oregon and California. Detailed matching of observed and theoretical seismograms is only possible if the effects of the source and recording are both introduced in the calculation of the theoretical waveform. Helmberger and Wiggins used an effective source time function obtained from recordings at ranges greater than 35°, where the arrivals are only slightly affected by the mantle structure. Despite the use of sources to the west and receivers mostly to the east of the Rocky mountains, which makes it rather unlikely that a laterally uniform model is appropriate, good fits were found to the observed seismograms. No allowance was made in this work for the effects of attenuation which, as pointed out by Kennett (1975b), has a strong influence on the final velocity model.

In past few years a number of large scale seismic refraction experiments along 1000 km lines with a dense system of calibrated receivers have been carried out in Western Europe. The design of these experiments has been influenced by the deep seismic sounding technique used in Eastern Europe for the determination of crustal structure. Major profiles have been conducted across France in 1971 (Hirn et al., 1973), which was reoccupied in 1973 with shifted shot point (Hirn et al., 1975). These profiles followed the axis of the old Amorican mountain system and show relatively uniform crustal structure (Sapin and Prodehl, 1973). However a profile along the length of the British Isles in 1974 (Bamford et al., 1976) crosses tectonic province boundaries and leads to a more complex pattern of variable crustal structure and depth to Moho.

The interpretation of these long range profiles has been based on initial travel time analysis supplemented by the calculation of theoretical seismograms to select the velocity structures which match the amplitude distribution along the profiles. Variations in ground coupling and ignorance of the true source time function preclude detailed matching of observed and theoretical seismograms along the profiles.

2. Interpretation Techniques

In this article we will discuss the interpretational techniques which can be used to try to determine the velocity structure from the observed seismograms and the assumptions which are built into these approaches. Unfortunately the real earth departs from the rather simple constraints which we would like to place on our models and we have therefore to examine the consequences of the deficiencies in our models. We will consider in particular the problems posed by the attenuation of seismic waves in their passage through the mantle and the influence of variations in the depth of the crust-mantle interface on the wavefield recorded at the surface.

The initial interpretation of a long range seismic profile must be based on the travel times of the seismic phases along the profile. The accuracy of this data is dependent on the ease of correlating a particular phase across an assemblage of seismograms. This process is normally not too difficult for clear first arrivals but can present considerable problems for later arrivals. The common procedure is then to find a velocity model for which calculated travel times are in agreement with the observed. This work is usually done by a process of trial-and-error fitting, and can be applied even if there are lateral variations in structure. For a model described by a limited number of parameters the approach can be systematised via a Monte-Carlo inversion technique. If it is reasonable to suppose that the structure is horizontally stratified, then the travel time data may be used in an extremal inversion approach devised by Bessonova et al. (1974) to set bounds within which the velocity distribution must lie. The separation of these bounds is determined by the accuracy of the original data. This approach has been applied to refracted wave data from long range profiles by Kennett (1976a) and Bates and Kanasewich (1976) and has recently been extended by Kennett (1977) to obtain bounds on the depths of reflectors from precritical reflections. In the course of this inversion the original travel time data are converted to an intercept time $\tau(p)$ relation as a function of ray parameter p. Jumps in $\tau(p)$ are diagnostic of velocity inversions, but the nature of this relation is entirely dependent on the correlations made on the original records. As pointed out by Hirn et al. (1975) the values of $\tau(p)$ just above a jump are based on the least accurate correlations so that the results have to be treated with caution.

In order to attempt to refine the initial models obtained from travel time analysis further use must be made of the information on the original seismograms and both the relative amplitude of arrivals on a single record and the amplitude distribution across a profile can be used as constraints. It is normally

most convenient to use this information by comparing theoretical seismograms, calculated for proposed velocity models, with the observations. If there are strong lateral variations in structure then the only suitable approach at present is to use asymptotic ray theory (Červený et al., 1974) but this is likely to be in error in the neighbourhood of critical points and caustics.

If the structure can be regarded as horizontally stratified then theoretical seismograms can be calculated by the reflectivity method introduced by Fuchs and Müller (1971) which has the advantage that for much of the structure all internal multiple reflections and interconversions can be included. The velocity model is represented as a stack of uniform layers of isotropic material. By introducing a complex velocity distribution, the effect of attenuation may also be introduced into the theoretical seismograms (Kennett, 1975b).

At the moment there is no direct method which may be used for the comparison of observed and theoretical seismograms and therefore visual inspection is used. Velocity models based on this approach tend to have rather smoother properties than those based on simple travel time analysis. However even the use of theoretical seismograms does not necessarily allow the definition of the details of the velocity distribution. Fuchs (1970) has demonstrated that a number of perfectly elastic models remain essentially indistinguishable if only post-critically reflected and refracted arrivals are considered. It is only if the precritical behaviour can be clearly distinguished that a further discriminant can be applied, but these later arrivals are difficult to trace. Attenuation also increases the potential ambiguity in the velocity structure as will be mentioned in the next section.

So far anisotropy has not been directly included in the calculation of theoretical seismograms although there is increasing evidence that it is present just below Moho on the continents (e.g. Bamford, 1973) and possibly also at greater depths (Hirn, 1977).

If the true velocity structure has lateral variations then the straightforward use of amplitude and travel time techniques based on the assumption of horizontal stratification will lead to bias in the proposed velocity models. We will consider these effects further in Sections 4 and 5 and consider in particular the effect of topography at the crust-mantle interface.

3. Attenuation versus Structure

The 1971 long range profile across France (Hirn et al., 1973) showed a relatively low apparent velocity of arrivals (around $8.20\,\mathrm{km\,s^{-1}}$) from 150 to 1000 km range, but with little decrease in amplitude. Close inspection reveals that this is acheived by the interaction of a number of phases. The P_n arrival propagating close to the crust-mantle interface is apparent from 150–250 km and is then superceded by a sequence of en echelon phases: P_{I} in the range 300–500 km, and P_{II} between 450–650 km. A further P_{III} phase beyond 600 km was correlated by Kind (1974). On the basis of the amplitude behaviour (Hirn et al., 1973; Kind, 1974) and also systematic travel time inversion (Kennett, 1976a, 1977) the

retrograde P_{I} and P_{II} branches are to be associated with transition zones in the mantle velocity distribution at depths of 50–60 km and 75–85 km. The shallower transition zone is overlain by a velocity inversion and a smaller second velocity inversion beneath this transition zone is also compatible with the data (Hirn et al., 1973; Kind, 1974).

Despite the strength of the retrograde P_{II} branch there is no clear indication of a corresponding prograde, refracted, branch. In consequence Kind (1974), who did not consider absorption, made the assumption of a further velocity inversion so that there was only a very weak refracted branch. As noted by Kennett (1976a), a similar effect may be produced by introducing attenuation into the velocity structure.

In Figure 1 we present a comparison of the effects of attenuation and structure based on the velocity models discussed by Kind (1974, Figs. 9, 10). Theoretical seismograms have been calculated allowing for attenuation within the velocity using a modified version of the reflectivity method (Kennett, 1975b). A phase velocity window from 8.0–10.0 km s^{-1} has been employed, so that Moho reflections $P_M P$ are not included. The basic source pulse used has a dominant frequency of 3.3 Hz.

Figure 1a shows a theoretical record section for a structure with well developed retrograde P_{I} and P_{II} phases but also a clear refracted branch (r) extending to the end of the calculated profile. The model is assumed to have a P-wave Q_α of 2000 except within the major velocity inversion where Q_α is dropped to 500, this acheives a shift in dominant frequency between the P_n (3.2 Hz) and $P_{\mathrm{I,II}}$ phases (2.8 Hz) comparable to that observed by Hirn et al. (1973). Figure 1b shows the record section correspond to the modified model proposed by Kind to explain the P_{I} and P_{II} branches, the same attenuation structure is assumed as in Figure 1a. The strong negative velocity gradient introduced beneath 80 km depth effectively eliminates any refracted arrival but at the cost of a more complicated velocity structure.

Figure 1c we present the record section corresponding only to a change of attenuation structure from that in Figure 1a. We have here assumed that in the lower transition zone and below Q_α again drops to the comparatively high value of 500. This has the result of considerably weakening the refracted arrival relative to the retrograde branch. Lower Q_α values would further reduce the size of the arrival. If we compare the record sections in Figures 1b and 1c we see that the general pattern of arrivals is very similar and the amplitudes differ by less than 20% out to a range of 650 km. Thus both velocity structure and attenuation can be effective in suppressing an unwanted arrival.

The weak refracted arrival in Figure 1c if interpreted in terms of a perfectly elastic structure would require a weak negative velocity gradient to exist below 80 km (cf. Hill, 1971). Thus by varying both the velocity gradient and the attenuation we can obtain a wide range of models with the same amplitude characteristics.

The models we have discussed represent extreme hypotheses as to the nature of the velocity structure along the profile, and it should be borne in mind that depatures from our assumption of lateral uniformity are likely to be of equal importance in the real situation.

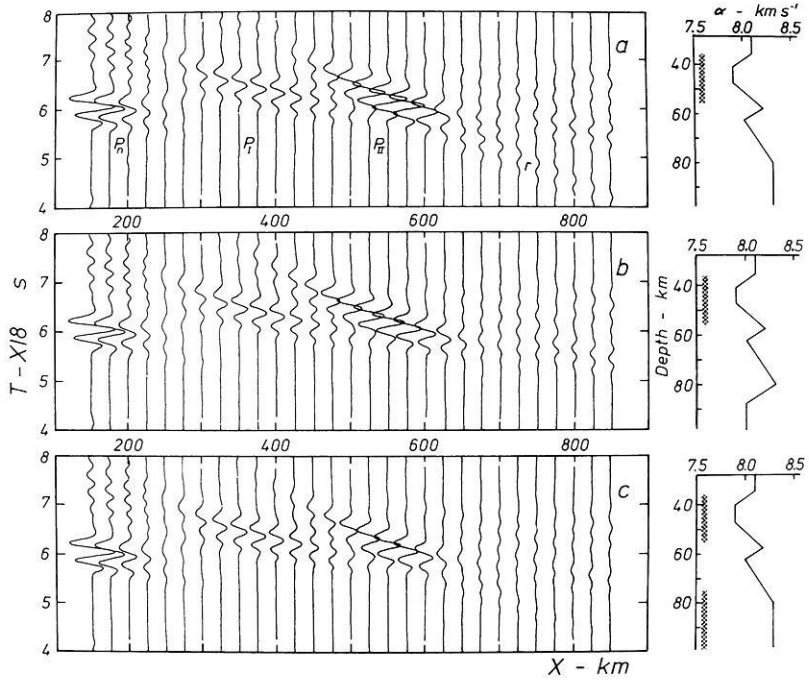

Fig. 1 a–c. Illustration of the effects of attenuation and velocity structure. The three sets of record sections of theoretical seismograms have been calculated for the velocity models shown on the right hand side, all of which have a 29 km crust with velocity 6.2 km s^{-1}. The velocity models are corrected for sphericity and have P wave Q_α of 2000 except in those regions marked by shading where Q_α is dropped to 500. **a** Model from Kind (1974), Figure 9. **b** Model from Kind (1974), Figure 10. **c** Alternative model with increased attenuation. No scaling is applied with range

The results of Steinmetz et al. (1974) from recordings of a ten ton shot off Western Scotland suggest that there is a velocity inversion below around 90 km depth, though the evidence is not so pronounced on other paths (Hirn, 1977). It is therefore likely that the failure to observe a refracted arrival at long ranges on the French profile is due to a combination of attenuation and velocity structure, which is not necessarily laterally uniform under the Auvergne (Perrier and Ruegg, 1973).

These results show that the final interpreted velocity distribution is strongly dependent on the form of the attenuation structure which is assumed. Further striking examples of this effect are presented in the work of Mellman and Helmberger (1974) and Fuchs and Schulz (1976) who have shown very close agreement between wave-leakage through a high speed lamina and an attenuative model.

4. Lateral Variation in Structure

In the most recent long range profiles on land (e.g. Bamford et al., 1976) a combination of short crustal refraction lines and reversed and overlapping long range lines should provide adequate coverage to examine deep lateral variations.

However in many earlier experiments and in those areas where such long range profiles are logistically very difficult, e.g. on the sea floor at continental margins or in the ocean basins, the level of data coverage available may well be only sufficient to delineate the variations in crustal structure along the profile. Particularly when a number of shots from a single shot point are recorded at large ranges by a mobile array of receivers (or as at sea where many shots are recorded at a single receiver site), there exists the possibility that there might well be some unrecognised lateral variation in the deep structure. The degree of bias introduced into systematic travel time inversions by lateral variations in mantle structure has been examined by Kennett (1976b), who used travel times calculated for a laterally heterogeneous velocity model in travel time inversion schemes designed to produce an "equivalent" horizontally stratified model fitting the data. Further numerical experiments of this type for modest levels of lateral heterogeneity in the mantle (e.g. about 2% variation in velocity at constant depth), using realistic estimates of the accuracy of observed travel times have shown that, if crustal effects can be removed, the equivalent horizontally stratified model lies within the envelope of uncertainty on the velocity distribution derived from extremal inversion.

Some bounds on the effect of lateral variations can be obtained from a comparison of overlapping profiles, where the same line of recording stations is occupied but with shifted shot point, unless there is significant change in crustal structure on the portion between the shot points. Hirn et al. (1975) have compared the overlapping 1971 and 1973 profiles in France and have shown that the upper mantle structure in Brittany varies little along the profile. In addition to determine the variation in structure out of the plane of the main profile they have also compared the recordings along a number of fan profiles radiating from a single shot point. For Brittany the uncertainty in the velocity distribution in a velocity transition zone $\alpha(z)$ across the region ($\Delta\alpha = \pm 0.1$ km s^{-1}, $\Delta z = \pm 4$ km) is about half that for an individual profile obtained from travel times alone (Kennett, 1976a). Despite the difficulty in acheiving true reversal when energy is returned from a number of different levels, profiles conducted in opposite directions along the same line also give a very useful control on the degree of lateral variation at depth along the line.

Since most of the interpretational techniques which are available to us yield horizontally stratified velocity structures, the common procedure when lateral variations are known to exist (e.g. in shallow crustal structure) is to correct the observed data to some laterally uniform reference structure. Such a procedure may readily be carried out for travel times by employing ray tracing through the actual and reference structures, but presents much greater difficulties for the amplitudes of seismic waves.

If the changes in crustal structure are fairly modest and local horizontal stratification can be assumed, then theoretical seismograms can be calculated by the modification to the reflectivity method suggested by Kennett (1975a). These seismograms may then be used in a direct interpretational scheme.

For more complicated structures we have to resort to numerical experiments to gauge the influence of different types of structure in our inversion schemes. The results of the LISPB experiment (Bamford et al., 1976) show considerable

variations in the depth of the crust-mantle interface along the length of the British Isles and in the next section we therefore look at the effect of variable topography at the Moho on the seismic wavefield.

5. Topography at the Crust-Mantle Interface

In a previous study (Kennett, 1976b) we have shown that even relatively mild variations in the slope of the crust-mantle interface lead to noticeable changes in the pattern of ray propagation through the mantle, and in consequence to a change in the wave amplitude observed at the surface.

In the appendix we develop a high frequency approximation which allows us to consider the effects of a slightly irregular crust-mantle interface and we here apply this approach to a model derived from that presented by Bamford et al. (1976) from the LISPB profile. To isolate the effects of topography, we have adopted a uniform crustal velocity of $6.36\,\mathrm{km\,s^{-1}}$ and assumed a basically horizontally stratified mantle structure, which is not proposed as an interpretation of the LISPB long range results but used only for the purpose of the numerical experiment.

The method we use is a modification of the reflectivity method and we take the reflection zone to consist of all the structure below Moho. As we mention in the appendix, we assume that the top of the reflection zone averages to the flat level assumed in the reference model (32.5 km). This means that there may be slight inaccuracies in the amplitude and timing of waves reflected at the underside of the interface. The dominant arrivals corresponding to diving waves will however be correctly represented.

The amplitude distance behaviour for our model is displayed in Figure 2, together with the form of the crust-mantle interface, for propagation from north to south and from south to north. The amplitudes are compared with those calculated for the laterally uniform reference model, and have been derived from the theoretical seismogram sections in Figure 3, which have been calculated using a phase velocity window from 8.1–$10.0\,\mathrm{km\,s^{-1}}$ in all cases. This window corresponds to purely propagating waves in the layer immediately below the crust-mantle interface and allows direct comparison between flat and perturbed mohography. The inclusion of evanescent waves by lowering the minimum phase velocity would enhance the relative amplitude of the P_n and P_{I} relative to P_{II}.

The results for the reference horizontally stratified velocity structure with a Moho depth of 32.5 km are represented by the solid circles in Figure 2, whilst open squares are used for propagation from north to south through the perturbed structure and open triangles for propagation from south to north. The most noticeable feature of the amplitude distance behaviour in Figure 2 is that the fluctuations introduced by mohography are in general fairly small and are often less than the typical variability in observed amplitudes. The offset distance from the Moho to the recording point at the surface is about 45 km for the phase velocities considered so that the relevant topography is offset from the appropriate amplitude symbol. For the P_n ($<220\,\mathrm{km}$) and P_{II} ($>450\,\mathrm{km}$) phases

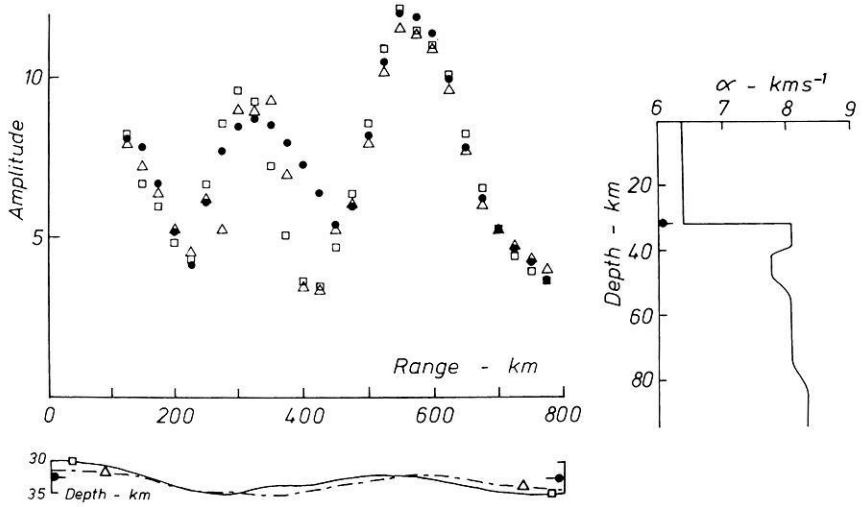

Fig. 2. Amplitude distance behaviour for topography on the crust-mantle interface, for phase-velocity window between 8.1 and 10 km s^{-1}. ● reference model illustrated at right with Moho depth of 32.5 km; □ propagation from North to South with topography on Moho illustrated at foot of diagram; △ propagation from South to North

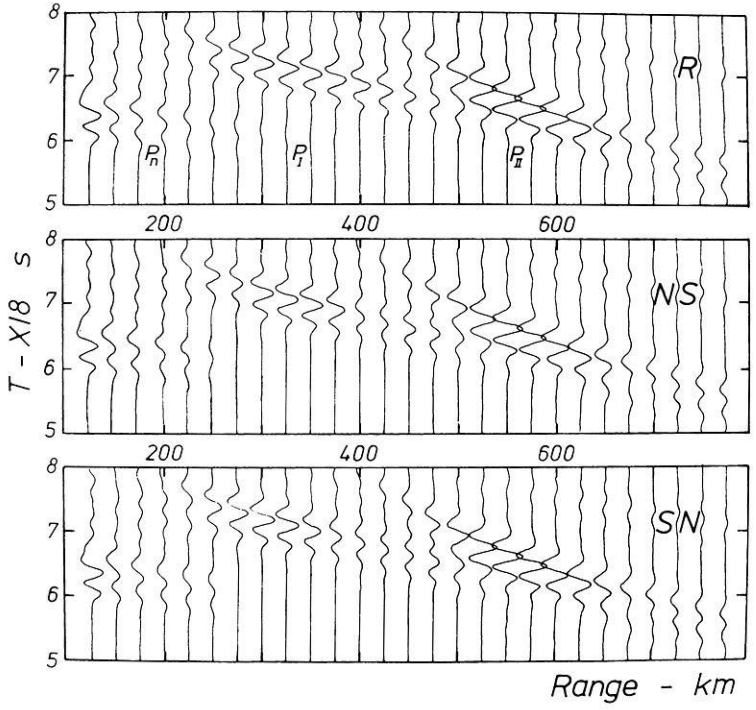

Fig. 3. Theoretical seismogram record sections illustrating the effect of topography at the crust-mantle interface. *R* reference structure; *NS* propagation from North to South; *SN* propagation from South to North. No scaling is applied with range

the effects of topography are small, but for P_I there are much greater differences between the 3 cases. Over the emergence range of this phase the two topographic profiles are broadly similar and both show a shift of the amplitude maximum to shorter ranges and a very pronounced amplitude minimum.

These features are clearly seen in the record sections of theoretical seismograms shown in Figure 3. The effect of topography is to produce a pronounced shift of energy to around 300 km and to give much reduced amplitudes just beyond 400 km. If we regard the NS and SN sections as being observed sections corrected for travel times, we see that the horizontally stratified velocity models which would be proposed to match these sections would differ markedly from the original reference model. In particular to shift energy to shorter ranges in the P_I phase a more pronounced velocity inversion would be required and to maintain the amplitude characteristics of the P_{II} phase the velocity would have to be increased between the two transition zones. Thus even for a basically laterally uniform mantle topography at the crust-mantle interface sufficiently alters the amplitude distribution along the profile so that, unless amplitude corrections are made, the interpreted velocity model will be distorted.

In general we have no guarantee that even the mantle structure is horizontally stratified and in this case it is important that as detailed corrections as possible are made to the amplitude and travel time of the observed phases to allow for the effects of known crustal variations. In this way we may hope to minimise the distortions in the final velocity model.

Acknowledgements. I have benefitted from useful discussions with many people during the course of this work, particularly with A. Hirn, D.H. Matthews, D. Bamford, K. Fuchs and S. Faber.

Appendix: The Effect of an Irregular Interface

We will calculate theoretical seismograms for a basically horizontally stratified medium containing a single irregular interface by an extension of the Kennett (1975a) modification of the reflectivity method (Fuchs and Müller, 1971). As before we consider the elastic half-space to be divided into 2 parts. In the lower region, the "reflection zone", all multiple reflections and interconversions are included by using efficient matrix techniques in the frequency and wavenumber domain, whilst above this region generalised ray theory is used. The seismograms are calculated by plane wave superposition.

In the case of a horizontally stratified medium, at a horizontal range X the vertical displacement at the surface $z=0$ is given by

$$W(X,t) = \int_{-\infty}^{\infty} d\omega\, \bar{S}(\omega) \exp(i\omega t)(\omega^2/\alpha_{\mathcal{M}}^2) \cdot \int_{\gamma_1}^{\gamma_2} d\gamma \sin\gamma \cos\gamma\, J_0(\omega X \sin\gamma/\alpha_{\mathcal{M}}) \cdot R_{pp}(\omega,\gamma)\, T_{\mathcal{D}}(\omega,\gamma)\, T_{\mathcal{U}}(\omega,\gamma) \quad (1)$$

where $\alpha_{\mathscr{M}}$ is the P wave velocity just above the reflection zone, $\bar{S}(\omega)$ is the source spectrum, $R_{pp}(\omega, \gamma)$ the reflection coefficient for the reflection zone, and $T_{\mathscr{D}}(\omega, \gamma)$, $T_{\mathscr{U}}(\omega, \gamma)$ are the overall transmission coefficients, including phase delays, from the surface to the reflection zone and from the reflection zone to the receiver. The integration variable is the angle of incidence at the top of reflection zone and the limits are specified by

$$\gamma_{1,2} = \sin^{-1}(\alpha_{\mathscr{M}}/c_{1,2})$$

where c_1 is the largest and c_2 the smallest phase velocity considered.

We take the irregular interface to lie at or just above the reflection zone and include its effects by calculating the redistribution of energy, due to the interface, across the plane waves at the regions where the band of phase velocities we are considering enter and leave the reflection zone. If the interface is taken to lie at the top of the reflection zone we assume that its long term average is flat so that the usual reflection coefficient may be used.

We are restricted in such an approach to considering interfacial topography of small amplitude whose horizontal scale is very much greater than the seismic wavelength. We specify the relief on the interface by the function $H(X)$ relative to a flat datum, with H measured positive upwards; it is convenient to use point values and then interpolate with a cubic spline. For a ray with ray parameter $p(=\sin\gamma/\alpha_M)$ the offset between the surface and the datum plane will be

$$\Delta X = \sum_{j=1}^{m} h_j \sin\gamma / [(\alpha_{\mathscr{M}}^2/\alpha_j^2) - \sin^2\gamma]^{\frac{1}{2}} \tag{2}$$

and for moderate relief the time correction introduced by the interface now being at $H(X)$ will be

$$\Delta Y(\gamma) = H(X_0)(1/\alpha_{\mathscr{M}})\{[(\alpha_{\mathscr{M}}^2/\alpha_{\mathscr{R}}^2) - \sin^2\gamma]^{\frac{1}{2}} - [1 - \sin^2\gamma]^{\frac{1}{2}}\} \tag{3}$$

where $\alpha_{\mathscr{R}}$ is the velocity below the interface and X_0 is the point of intersection of the ray and the datum. Such a time correction will need to be introduced at both the points of entry and exit of a ray at the reflection zone. In addition the slope of the interface will lead to a change in the effective angle of incidence of the ray at the datum plane.

We introduce the slope of the interface

$$\vartheta(X) = \tan^{-1}(H'(X)) \tag{4}$$

and then the effective angle of incidence in the layer above the top of the reflection zone γ_e, defined as the angle of incidence in the medium $\alpha_{\mathscr{M}}$ for a flat interface which corresponds to the ray in the medium $\alpha_{\mathscr{R}}$ in the case of the inclined interface, is given by: on entry

$$\gamma_e = \sin^{-1}[(\alpha_{\mathscr{M}}/\alpha_e)\sin\{\vartheta + \sin^{-1}[(\alpha_{\mathscr{R}}/\alpha_{\mathscr{M}})\sin(\gamma - \vartheta)]\}] \tag{5}$$

and on exit

$$\gamma_e = \sin^{-1}[(\alpha_{\mathscr{M}}/\alpha_{\mathscr{R}})\sin\{\vartheta + \sin^{-1}[(\alpha_{\mathscr{R}}/\alpha_{\mathscr{M}})\sin\gamma]\}] - \vartheta \tag{6}$$

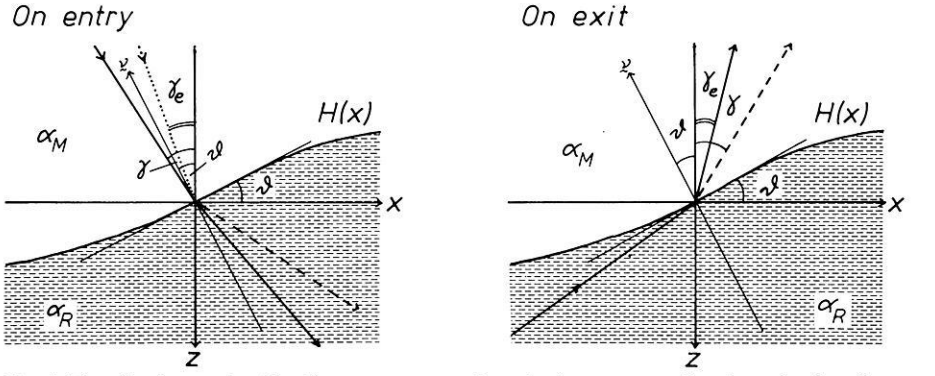

Fig. 4. The effective angle of incidence γ_e, ⟶ Rays in the presence of an irregular interface; — → — Rays for a flat interface; ···→··· Effective ray

in which ϑ is a function of γ through Equations (2) and (4). The angles γ_e correspond to the incident angles appropriate to the energy actually propagating in the reflection zone. Hence in the case of an irregular interface the angular integration in Equation (1) should be taken over the γ_e. However we may change back the variable of integration to the original variable γ by the mappings: on entry to the reflection zone

$$d\gamma_e = A_{\mathscr{D}}(\gamma)\, d\gamma \tag{7}$$

and on exit

$$d\gamma_e = A_{\mathscr{U}}(\gamma)\, d\gamma. \tag{8}$$

These mappings represent the redistribution across the plane wave spectrum due to the irregular interface. In addition we need to take into account the differential phase delays between the various plane waves introduced by the variation in the position of the interface.

We may therefore introduce the effects of topography at the top of the reflection zone into the scheme for calculating the theoretical seismograms (Eq. (1)) by modifying the transmission terms $T_{\mathscr{D}}(\omega, \gamma)$, $T_{\mathscr{U}}(\omega, \gamma)$ to take account of the redistribution across the plane waves due to the interface and the differential phase delays. Thus in Equation 1 we substitute $B_{\mathscr{D}}(\omega, \gamma)$ and $B_{\mathscr{U}}(\omega, \gamma)$ for $T_{\mathscr{D}}(\omega, \gamma)$ and $T_{\mathscr{U}}(\omega, \gamma)$ where

$$\begin{aligned} B_{\mathscr{D}}(\omega, \gamma) &= T_{\mathscr{D}}(\omega, \gamma)\, A_{\mathscr{D}}(\gamma) \exp[-i\omega \Delta t_{\mathscr{D}}(\gamma)] \\ B_{\mathscr{U}}(\omega, \gamma) &= T_{\mathscr{U}}(\omega, \gamma)\, A_{\mathscr{U}}(\gamma) \exp[-i\omega \Delta t_{\mathscr{U}}(\gamma)] \end{aligned} \tag{9}$$

and $\Delta t_{\mathscr{D}}(\gamma)$ and $\Delta t_{\mathscr{U}}(\gamma)$ are the time corrections on entry to and exit from the reflection zone.

Although the mappings $A_{\mathscr{D}}(\gamma)$ and $A_{\mathscr{U}}(\gamma)$ could be derived analytically from Equations (5) and (6) the rather involved functional dependence of ϑ on γ makes this procedure unattractive computationally. We therefore use a discrete form of calculation to determine the weighting functions $A_{\mathscr{D}}(\gamma)$ and $A_{\mathscr{U}}(\gamma)$.

To calculate the inner integral in Equation (1) we employ a discrete set of N values of the angle γ, and for each of these we calculate the effective angles for

both entry and exit, which do not necessarily fall on the preassigned values of γ. In order to avoid the instability associated with simple differentiation by differences we adopt a stable, N-point smoothing approach. For each of the γ_e we assign to each discrete value of γ_i the $(\sin x/x)$ weight appropriate to a band limited N sample representation of a delta function at γ_e. We then sum these weights for each discrete γ_i to generate the distributions $A_{\mathscr{D}}(\gamma_i)$, $A_{\mathscr{U}}(\gamma_i)$ which are then used in the calculation. For a flat interface this scheme has the required property of yielding unit distributions.

References

Bamford, D.: Refraction data in Western Germany – a time term interpretation. Z. Geophys. **39**, 907–927, 1973

Bamford, D., Faber, S., Jacob, B., Kaminski, W., Nunn, K., Prodehl, C., Fuchs, K., King, R., Willmore, P.: A lithospheric seismic profile in Britain I – Preliminary Results. Geophys. J. **44**, 145–160, 1976

Bessonova, E.N., Fishman, V.M., Ryaboyi, V.Z., Sitnikova, G.A.: The tau method for the inversion of travel times – I Deep seismic sounding data. Geophys. J. **36**, 377 – 398, 1974

Bates, A.C., Kanasewich, E.R.: Inversion of seismic travel times using the Tau method. Geophys. J. **47**, 59–72, 1976

Červený, V., Langer, J., Pšenčík, I.: Computation of geometric spreading of seismic body waves in laterally inhomogeneous media with curved interfaces. Geophys. J. **38**, 9–20, 1974

Fuchs, K.: On the determination of velocity depth distributions of elastic waves from the dynamic characteristics of the reflected wave field, Z. Geophys. **36**, 531–548, 1970

Fuchs, K., Müller, G.: Computation of synthetic seismograms by the reflectivity method and comparison with observations. Geophys. J. **23**, 417–433, 1971

Fuchs, K., Schulz, K.: Tunneling of low frequency waves through the subcrustal lithosphere. J. Geophys. **42**, 175–190, 1976

Hales, A.L.: The travel times of P seismic waves and their relevance to the upper mantle velocity distribution. Tectonophysics **13**, 447–482, 1971

Helmberger, D.V., Wiggins, R.A.: The upper mantle structure of the mid-western United States. J. Geophys. Res. **76**, 3229–3245, 1971

Hill, D.P.: Velocity gradients and anelasticity from crustal body wave amplitudes. J. Geophys. Res. **76**, 3309–3325, 1971

Hirn, A., Steinmetz, L., Kind, R., Fuchs, K.: Long range profiles in Western Europe II-Fine structure of the lower lithosphere in France (Southern Bretagne). Z. Geophys. **39**, 363–384, 1973

Hirn, A., Prodehl, C., Steinmetz, L.: An experimental test of models of the lower lithosphere in Bretagne (France). Ann. Géophys. **31**, 517–530, 1975

Hirn, A.: Anisotropy in the continental upper mantle: possible evidence from explosion seismology. Geophys. J. (in press)

Iyer, H.M., Pakiser, L.C., Stuart, D.J., Warren, D.H.: Project Early Rise: seismic probing of the upper mantle. J. Geophys. Res. **74**, 4409–4441, 1969

Jeffreys, H.: On near earthquakes. MNRAS Geophys. Suppl. **1**, 385–402, 1926

Kennett, B.L.N.: Theoretical seismogram calculation for laterally varying crustal structures. Geophys. J. **42**, 579–589, 1975a

Kennett, B.L.N.: The effect of attenuation on seismograms. Bull. Seism. Soc. Am. **65**, 1643–1651, 1975b

Kennett, B.L.N.: A comparison of travel time inversions. Geophys. J. **44**, 517–536, 1976a

Kennett, B.L.N.: The effect of lateral variations on seismic refraction interpretation. Pageoph. **114**, 647–652, 1976b

Kennett, B.L.N.: The inversion of reflected wave travel times. Geophys. J. **49**, in press

Kind, R.: Long range propagation of seismic energy in the lithosphere. Z. Geophys. **40**, 189–202, 1974

Mellman, G.R., Helmberger, D.V.: High frequency attenuation by a thin high velocity layer. Bull. Seism. Soc. Am. **64**, 1383–1388, 1974

Mohorovičić, A.: Das Beben vom 8.10.1909, Jahrb. Meteorol. Obs. Zagreb für 1909, **9**, 4 Abschnitt 1

Perrier, G., Ruegg, J.C.: Structure profonde du Massif Central français. Ann. Géophys. **29**, 435–502, 1973

Sapin, M., Prodehl, C.: Long range profiles in Western Europe I—Crustal structure between the Bretagne and the Central Massif of France. Ann. Géophys. **29**, 127–145, 1973

Steinmetz, L., Hirn, A., Perrier, G.: Réflexions sismiques à la base de l'asthénosphère. Ann. Géophys. **30**, 173–180, 1974

Wiggins, R.A., Helmberger, D.V.: Upper mantle of the western United States. J. Geophys. Res. **78**, 1869–1880, 1973

Received October 15, 1976; Revised Version January 7, 1977